JPMTR 128 | 1912
DOI 10.14622/JPMTR-1912
UDC 774.8-024.25-021.383|004.02

Original scientific paper
Received: 2019-11-27
Accepted: 2019-12-31

Prediction of lamination-induced colour shifts for UV offset printings by using a heuristic approach as well as machine learning techniques

Tim Stiene, Peter Urban and Jorge Manuel Rodriguez-Giles

University of Wuppertal,
School of Electrical, Information and Media Engineering,
Rainer-Gruenter-Straße 21, D-42119 Wuppertal

stiene@uni-wuppertal.de
purban@uni-wuppertal.de
albaodila@hotmail.com

Abstract

To investigate two approaches for the prediction of spectral colour changes, UV offset-printed test charts were laminated with polybutylene terephthalate films in three thicknesses and measured spectrophotometrically before and after lamination. This enabled the identification of the resulting colour shift for each patch. Mean colour deviations of 3.4 ΔE_{00} were determined while the strength of a colour shift depended on the initial colour patch lightness and the presence of paper white. To predict spectral reflections, a heuristic approach, based on the calculation of wavelength-dependent transmission of the lamination, is presented. A mean accuracy of 1.44 ΔE_{00} between predictions and actual measured coated reflections was achieved. The method still shows potential for improvements in the prediction of the paper white after lamination. In a second approach, an artificial neural network (ANN) was applied to evaluate the performance of machine learning on this topic as well. After training and validation, using the ANN for spectral prediction led to a higher precision with a mean ΔE_{00} of 0.6. In conclusion, both approaches obtain useful results whereby the ANN predictions are significantly more accurate. The investigation also demonstrates the potential of machine learning in the field of print and media technologies in general and in colour science in particular.

Keywords: colour difference, spectral prediction, lamination, neural network, colour measurement

1. Introduction and background

To meet the requirements of an increasingly specialised printing market, a large number of printed products are finished achieving various physical properties for optical as well as barrier characteristics. Main surface finishing techniques are lamination and varnishing, which one could summarise under the term 'coating'. It is known that coatings can affect the colour appearance of print products due to a number of optical effects that occur on interfaces between coating layer(s), printed ink(s) and substrate. Important coating-related optical phenomena are scattering, reflection, absorption and refraction, which can significantly influence the visible or measurable reflection (Galić, Ljevak and Zjakić, 2015). Modified colour appearances can be caused by multiple reflections between print and coating and/or scattering depending on surface roughness. Also relevant in this regard is light trapping during colour measurements caused by coating-induced change of the distance between measurement device and colour patch. To visualise these colour shifts, Figure 1 shows scanned CMYK wedges whose lower half is coated manually with a glossy film. Differences in colour appearance can be seen between coated and uncoated colours. This effect is particularly apparent for medium area coverages.

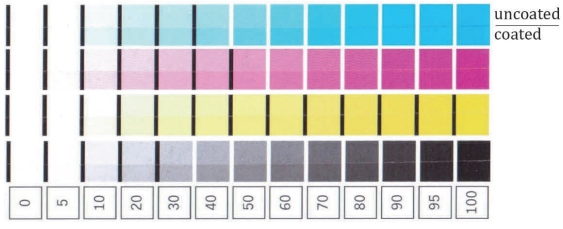

Figure 1: Digital scan of UV offset CMYK wedges (printed in 80 l/cm AM screening), 13 patches per wedge in nominal tone values from 0 % to 100 %, the lower half of each wedge is coated with glossy film

The colour change is attributed to a measurable coating-induced dot gain in many studies, i.e. by Gemeinhardt, Saba and Skoczowski (2009). It is also known that glossy coatings cause more saturated colour appearances while matte coatings result in more faded colours and decreased colour gamuts (Childers, et al., 2008). This can be attributed to the influence of surface reflected light on the measurements. In case of glossy surfaces, only a small quantity of these reflections reaches the sensor under 45°/0° geometry as opposed to matte coatings, where scattering leads to a larger amount of light reaching the sensor. Since surface reflections do not carry colour information of the print, the measured colours appear as mentioned (Gemeinhardt, Saba and Skoczowski, 2009).

Besides physical properties of coating materials, these optical phenomena are also affected by print specifications such as the substrate and screening used (Hoffstadt, 2004). In case of substrates containing optical brighteners, UV-absorbing coatings could attenuate the excitation of optical brighteners and, thus, their fluorescence emission. Applying UV-cured varnishes can also have a significant influence on colour appearance due to their specific polymerisation-induced yellowing properties. However, the two latter phenomena must be considered separately since they differ from the classic optical effects mentioned above. Any kind of reflection modification can naturally lead to visible and measurable colour deviations between the standard-conforming printing results and the finally coated products.

Keeping processes controllable and results predictable is of fundamental importance in print productions. While the press operator still has influence on the final colour appearance in case of inline coatings, this option is not available for post-press coating. This resulted in the development of a variety of approaches to examine or predict coating-induced colour shifts. Those approaches relevant for the object of this paper will be presented briefly in the following. As a very practical tool for print productions, *Fogra49* resp. *Fogra50* introduces special ICC profiles to generate coating proofs for matte and glossy OPP (oriented polypropylene) film laminations with regard to sheetfed offset (Kleeberg, et al., 2018). These proofs are intended to simulate only the final visual appearance to simplify colour communication in print productions. Galić, Ljevak and Zjakić (2015) focused on the characterisation of varnish-influenced colour shifts on spot colours using different substrates and found significant colour changes of $\Delta E_{00} > 2$ for all glossy UV-coated samples. Hoffstadt (2005) describes an approach using modified ICC profiles: for each coated patch, a colorimetric counterpart in the uncoated profile must be identified and both be connected with modified gradation curves to predict the colour appearances for coated colour patches on this basis. By doing so, Hoffstadt reaches predictions with a mean accuracy from 1.5–1.7 ± 0.6 ΔE^*_{94} compared to initial colour shifts ranged from 3.4–4.0 ± 1.2 mean ΔE^*_{94} for various glossy coatings. Hébert, Emmel and Hersch (2002) adapt existing reflectance models for the specific requirements of varnished metallic plates as a first step for further improved prediction methods.

In our work, two new spectral-based approaches to predict lamination-induced colour shifts are presented. The first is a heuristic one, the second applies machine learning techniques. In addition, both approaches will be compared in terms of their attainable accuracy and practical potential.

2. Methods

2.1 Sample preparation and measurement settings

To evaluate both approaches, adapted EFI Fiery profiling charts IT8 i1IO with 936 patches (Figure 2) were printed with a Heidelberg Speedmaster 52-4+L UV Anicolor in 80 l/cm AM screening. Printing was done with Heidelberg Anicolor UV LM Process Inks in KCMY sequence on a glossy CHROMOLUX 700 215 g/m^2 substrate, which has a faint fluorescence emission of 1.3 Δb_{00}. The fluorescence emission is determined as the difference Δb^* between M2 and M1 measurements, using a Konica Minolta FD-7 spectrodensitometer with D50 illuminant and 2° CIE standard observer. Lamination of the sample was implemented with polybutylene terephthalate (PBT) lamination film from the manufacturer Richter & Menzel in thicknesses of 42 µm, 75 µm and 125 µm using an offline laboratory laminating device in operating temperature of 70 °C. Three samples were measured spectrophotometrically before and after lamination using a Konica Minolta FD-9 Auto Scan spectrophotometer in 45°/0° geometry, M1, D50 illuminant, 2° CIE standard observer, 10 $\Delta\lambda$ (wavelength pitch), 3 mm measuring spot configuration. Each patch was measured on 2 spots, and 4 times in total. For evaluation and comparison, the reflection spectra were converted to the CIELAB colour space and colour deviations were expressed in CIEDE2000 (ΔE_{00}) (International Organization for Standardization / International Commision on Illumination, 2014).

2.2 Heuristic approach

The heuristic approach calculates uncoated reflection spectra with the transmission of a lamination, which is also adjusted for corrected area coverages of each colour separation. It does not follow a physical model but takes into account some observations one could make based on Figure 1. One can see that the colour shift

Figure 2: EFI profiling chart IT8 i1IO (originates from software EFI Fiery XF 6), 936 randomised patches in 39 columns and 24 rows, patch size 7 mm × 9 mm, printed in 32 cm × 23 cm

depends on the presence of unprinted paper white. This is presumably caused by coloured back reflections which are mostly noticeable on paper white. For further improvement, the lamination's specific surface reflection is added. In the following, the approach with its related calculations are presented, beginning with the necessary symbols.

$R(\lambda)$	spectral reflection over 380–730 nm
$\Delta R(\lambda)_{\text{surface}}$	difference in spectral surface reflection without colour information, measured at a dark colour patch
$T(\lambda)$	spectral transmission over 380–730 nm
AC_{nom}	nominal area coverage, acquired from printing data for each colour separation of each patch
AC_{corr}	calculated corrected area coverages for each colour separation of each patch
n	exponent for adjustment of $T(\lambda)$
f, k	parameters for fitting

Spectral transmission $T(\lambda)$, the quotient of printed colours and the blank substrate reflection gives the transparency of the ink layer of each patch by Equation [1]:

$$T(\lambda) = \frac{R(\lambda)_{\text{patch unlaminated}}}{R(\lambda)_{\text{substrate unlaminated}}} \qquad [1]$$

The sinus in Equations [2] to [5] represents the sinusoidal course of the dot gain as it is lowest at areas of small and high area coverages and highest in the range of medium area coverages. Therefore, Equation [6] considers the amount of paper white for each patch.

Corrected area coverage AC_{corr} must be calculated separately for each colour separation of each patch using Equations [2] to [5].

$$AC_{\text{corr,C}} = [1 - T(\lambda)] \cdot \left[AC_{\text{nom,C}} + f \cdot \sin\left(\pi \cdot AC_{\text{nom,C}}\right)\right] \qquad [2]$$

$$AC_{\text{corr,M}} = [1 - T(\lambda)] \cdot \left[AC_{\text{nom,M}} + f \cdot \sin\left(\pi \cdot AC_{\text{nom,M}}\right)\right] \qquad [3]$$

$$AC_{\text{corr,Y}} = [1 - T(\lambda)] \cdot \left[AC_{\text{nom,Y}} + f \cdot \sin\left(\pi \cdot AC_{\text{nom,Y}}\right)\right] \qquad [4]$$

$$AC_{\text{corr,K}} = [1 - T(\lambda)] \cdot \left[AC_{\text{nom,K}} + f \cdot \sin\left(\pi \cdot AC_{\text{nom,K}}\right)\right] \qquad [5]$$

The exponent n, calculated by Equation [6], is for adjustment of $T(\lambda)$ and refers to the calculation of corrected area coverages AC_{corr}.

$$n = k\left[\left(1 - AC_{\text{corr,C}}\right) \cdot \left(1 - AC_{\text{corr,M}}\right) \cdot \left(1 - AC_{\text{corr,Y}}\right) \cdot \left(1 - AC_{\text{corr,K}}\right)\right] \qquad [6]$$

The $\Delta R(\lambda)_{\text{surface}}$ represents the differences in surface reflection between coated and uncoated patches and is determined exemplarily for a dark colour patch by Equation [7]. As the surface reflected light did not penetrate into the laminated sample but reflected directly without changes in spectral distribution from the surface, it is assumed as being free of colour information.

$$\Delta R(\lambda)_{\text{surface}} = \frac{R(\lambda)_{\text{patch unlaminated}}}{R(\lambda)_{\text{patch laminated}}} \qquad [7]$$

Following the heuristic approach, the spectral reflection after lamination is calculated by Equation [8]:

$$R(\lambda)_{\text{predicted}} = R(\lambda)_{\text{unlaminated}} \cdot T(\lambda)^n + \Delta R(\lambda)_{\text{surface}} \qquad [8]$$

The calculation method is set up in accordance with the equations with freely chosen start values for k and f and the resulting colour differences ΔE_{00} between $R(\lambda)_{\text{predicted}}$ and $R(\lambda)_{\text{laminated}}$ are calculated. Now, factors k and f must be fitted by minimising the mean ΔE_{00}. In this work, fitting is done by using the MS Excel Solver with the Generalized Reduced Gradient – GRG nonlinear solving method. However, it would be just as feasible to use any other numerical-analysis software one is familiar with. Once calculated for the specific print and lamination parameters, k and f can be used to make further spectral predictions. To enhance evaluation, only 80 % of all colour patches (749 patches per chart) are considered for fitting while the remaining 187 'unknown' patches of each chart are used as start and target data for predictions generated by both approaches to enable comparability. As the chart is already randomised, we simply take the desired number of patches starting at patch 1 (position 1A) line by line for each approach.

2.3 Artificial neural network approach

An artificial neural network (ANN) was set up to realise and examine colour shift prediction applying machine learning techniques. Generally, ANNs can be understood as a technical implementation of machine learning within technologies of artificial intelligence. For the purpose of this paper, ANNs are seen as an existing tool for solving a specific task in research. As it is more important to describe the basic functional principle and the actual setup of the network used than to explain the technical and mathematical principles of ANNs in detail, which are widely described in relevant literature (Hagan, et al., 2014; Chollet, 2018), only a brief explanation of the ANN fundamentals is given here.

Figure 3 shows the schematic architecture of a fully connected multilayer feedforward network which consists of three layers (input layer, hidden layer, output layer) with n number of nodes, the so-called 'neurons'. Every neuron represents a single computing unit and, in case of fully connected networks, is connected to all previous and subsequent nodes by weighted connections represented by matrices v and w. The number of input nodes must be chosen in accordance with the character of input data, the output nodes must comply with the output data. In this particular case, both the input and output have 36 nodes because the data sets consist of spectral data with 36 digits each (380–730 nm spectral range in 10 $\Delta\lambda$ wavelength pitch). The hidden layer setting must be chosen and has some

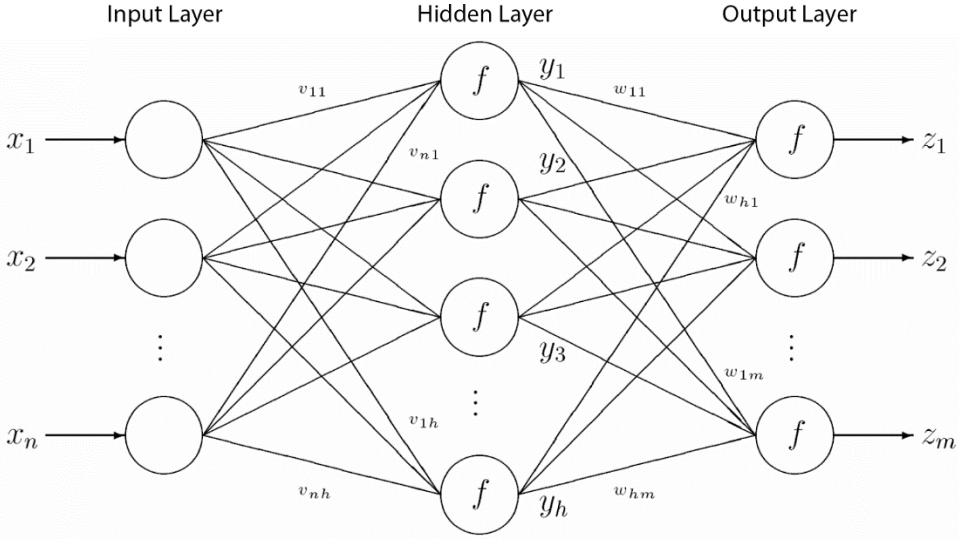

Figure 3: Schematic representation of a triple-layered artificial neural network with input x, hidden y and output layer z, weighted connections v and w and activation function f (Selle, 2018)

influence on the learning and results quality. To apply an ANN to a specific task, it is necessary to first train it using known examples of the problem to be solved. The process used for the purposes of this paper was 'supervised learning': by feeding the ANN with initial input data and related target data, it can learn that a specific input leads to a specific output.

Consequently, the training process requires sets of start and target data, which need to be split into sets of training (in this case: 70 %) and validation data (10 %). Furthermore, it is important to withhold test data (20 %) to ensure generalisation after training. Generalisation is the capability of a trained ANN to perform on unknown data from the same type as well as it does on the training data. On the other hand, memorisation or overfitting means the exact opposite: the ANN only remembers specific training targets but fails on unknown samples. (Hagan, et al., 2014)

As the test charts are already randomised, all colours in different combination of area coverages were considered. The learning process involves the feed-forward data processing and the backpropagation mechanism for an automatic weight adjustment. During feed-forward processing, the input data is processed through the network. For each neuron, its single input is calculated from all incoming values considering the weights. By a so-called 'activation' the input leads to a specific output which is processed to the subsequent nodes up to final outputs z_1 to z_m. (Chollet, 2018)

The resulting output error at each node is calculated by comparison with the actual target data. Now, using the method of backpropagation, the errors are propagated backwards into the ANN and the weights are adjusted in an automated process to minimise the output loss for each node, starting with the output layer. The direction of weight modification is identified by using the gradient descent approach. Feed-forwarding the inputs and backpropagation of resulting errors with weight adjustments jointly form a so-called 'epoch'.

The entire training routine usually consists of numerous epochs to successively minimise the output losses. The learning rate defines the intensity of the weight adjustments whereas the batch size specifies the number of processed single data between two weight adjustments. To evaluate the ANN's performance after training, the test data set can be used as input data for which the network should predict the corresponding target.

The Python programming language is used to set up an ANN based on the Keras framework (version 2.2.4). Keras is a high-level API (application programming interface) for Googles TensorFlow backend (version 1.12.0) and, as well as Python and all other software components used for implementing the ANN, available as open source software. For detailed information about possible functions and configurations, the authors refer to the relevant literature. (Hagan, et al., 2014; Chollet, 2018)

Besides a suitable data base and its proper preprocessing, the obtained performance of an ANN depends on actual realisation and task-specific adaption of all parameters (Chollet, 2018). The detailed setup and training configuration of the ANN used are summarised in Table 1 and Table 2, respectively. Apart from the parameters listed in the tables, the default settings for the given Keras version are used.

Table 1: Setup of the Keras-based ANN

Parameter	Input layer	Hidden layer	Output layer
Nodes	36	18	36
Activation func.	Hard sigmoid	Softmax	*default*

Table 2: The ANN training configuration

Parameter	Setup
Optimiser	Adam
Loss function	Mean square error
Learning rate	0.01
Epochs	2 000
Batch-size	2

3. Results

3.1 Short presentation of lamination-induced colour shifts

First, the obtained lamination-induced colour shifts are to be outlined. In the course of this paper, 'colour shift' means any modification in the spectral reflection. The findings presented in the following are always valid for all lamination thicknesses unless the contrary is noted. Looking at the spectral characteristics of coated and uncoated colours, significant lamination-induced colour shifts are revealed. Figure 4 exemplarily shows four spectral reflections of cyan in nominal area coverages of 20, 60, 80, and 100 % (C100 = cyan in 100 % nominal area coverage) and their corresponding coated reflection spectra. The shown spectra were selected in order to show differences in solid and halftone printed colours. While C100 shows only slight deviations (0.9 ΔE_{00}), the other patches show increasing colour shifts with increasing presence of blank paper white (0.9–4.0 ΔE_{00}).

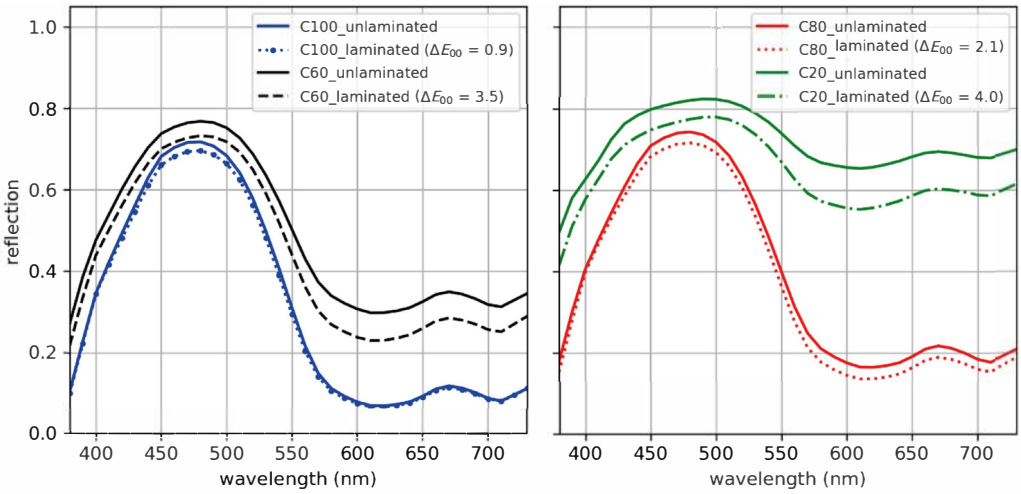

Figure 4: Spectral colour shift due to lamination with a 42 µm PBT film, exemplarily shown for reflection spectra of cyan in nominal area coverages of 100, 80, 60 and 20 %, in two graphs for better clarity

Since a rising presence of paper white is usually accompanied by an increasing brightness of a colour patch, a link between colour brightness and resulting colour shift can be assumed.

To verify this, Figure 5 shows the L^* values of an entire colour chart and resulting ΔE_{00} values after 42 µm lamination. It can be clearly seen that in areas of low lightness there is the smallest colour shift while it first increases at lighter colours and tends to have its spectral maximum in areas of medium lightness. Figure 6 shows changes in lightness between unlaminated and laminated colour patches, expressed in ΔL_{00}. To obtain a clearly arranged diagram, both the L^* and ΔL_{00} values were averaged in lightness intervals of 10 (arithmetic mean of all L^* values between 100 and 90, etc.) and spline interpolated with curves using Python's SciPy library with *interp1d* function. The curves correspond quite well with the scatter plot distribution in Figure 5.

This indicates not only that the resulting colour shift depends on colour lightness, but also that it is mainly caused by changes in lightness due to lamination. Furthermore, significant differences in lightness modification between the thickest and the two thinner films can be seen for areas of medium and high reflections.

For CIE chroma and hue, no connection can be found between these colorimetric characteristics and colour shifts. It is also noted that the laminations do not affect the substrates fluorescence emission which still has a value of 1.3 Δb_{00}. In conclusion, lamination does result in a significant colour shift, the size of which is principally related to colour patch lightness, in other words, the presence of paper white. In the following section, it will be discussed whether the approaches mentioned above can make useful spectral predictions.

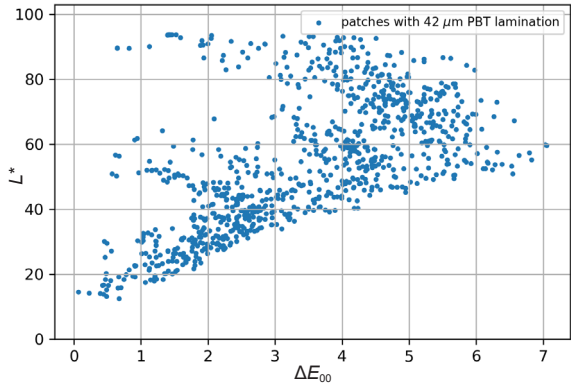

Figure 5: Relationship between lightness L for 936 unlaminated colour patches and corresponding lamination-induced colour shifts in ΔE_{00} due to lamination with 42 µm PBT film*

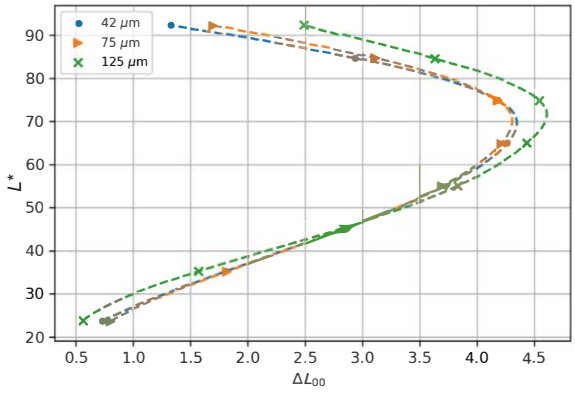

Figure 6: Relationship between lightness L (arithmetic mean values in intervals of 10) for 936 unlaminated colour patches and corresponding mean lamination-induced shifts in lightness ΔL_{00} due to lamination with 42, 75 and 125 µm PBT films; curves are spline interpolated*

3.2 Spectral predictions by both approaches

As described in the Section 2, factors *f* and *k* must be fitted for each specific lamination to adjust the heuristic approach. For fitting purposes, only 80 % of the data set (749 patches per chart) is considered – thus, predictions can be made for 'new' data. Table 3 shows the relevant fitting results for each lamination.

Table 3: Optimised correction factors f and k for each lamination

Lamination thickness [µm]	*f*	*k*
42	6.60	0.46
75	5.56	0.41
125	12.02	0.44

Next, selected spectral reflections with related predictions will be shown to give an impression about the performance of both approaches. Figure 7 shows four reflection spectra of coated patches and the predicted reflections using the heuristic approach. Figure 8 provides the same scenario for the ANN. The nominal area coverages for each spectrum are indicated as well as the achieved prediction accuracy in ΔE_{00} while the specific numbering c1, c2, c3 is of no significance. With regard to Figure 7, the heuristic approach gives good results for colour spectra. Weaknesses become visible for the paper white prediction which does not differ from the measured uncoated spectrum and the calculation method seems to have no impact. In the interest of completeness, it is noted that no functional interrelation between the colorimetric parameter lightness *L**, hue *h*, chroma *C** and the achieved prediction accuracies could be found during analysis.

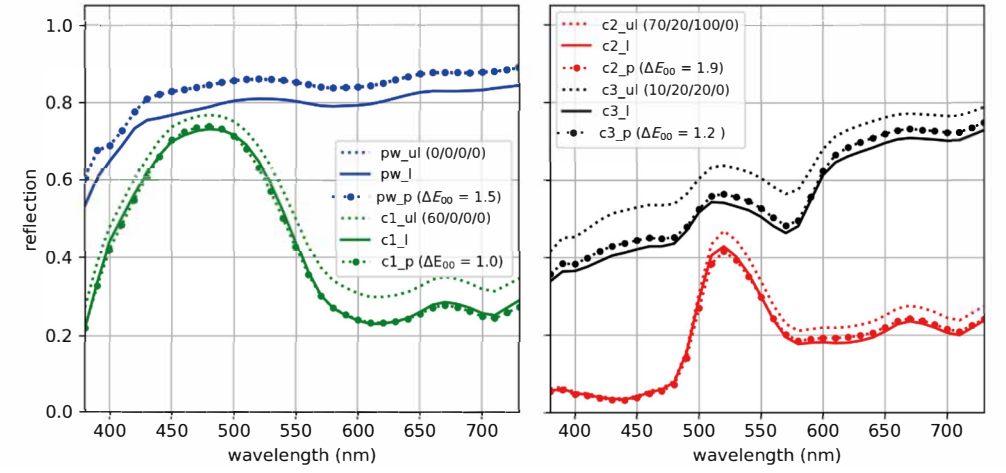

Figure 7: Laminated (l) and unlaminated (ul) reflection spectra for four patches (nominal area coverages expressed with C/M/Y/K in percent) with related spectral predictions (p) and their accuracies in ΔE_{00} by the heuristic approach for 42 µm PBT lamination

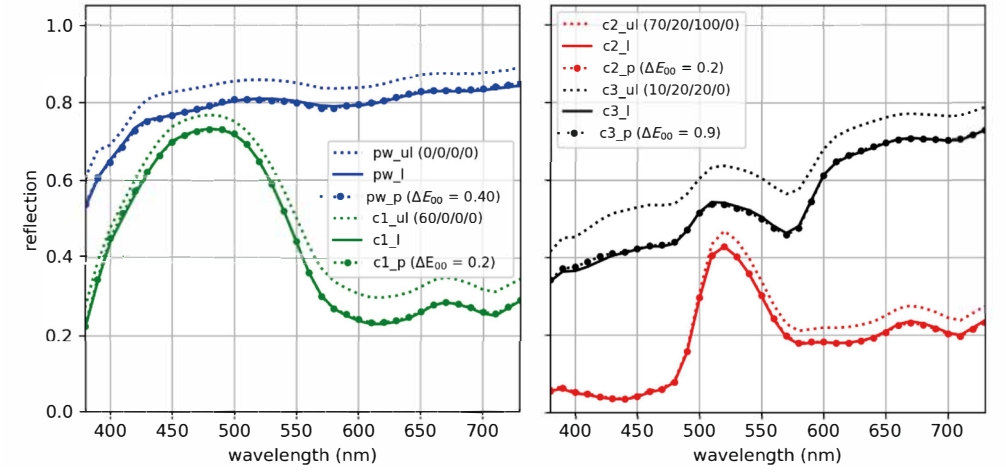

Figure 8: Laminated (l) and unlaminated (ul) reflection spectra for four patches (nominal area coverages expressed with C/M/Y/K in percent) with related spectral predictions (p) and their accuracies in ΔE_{00} by the neural network approach for 42 µm PBT lamination

Table 4: Final results for both approaches: initial colour shifts and prediction accuracies in arithmetic mean $\bar{x}\,\Delta E_{00}$ and 90th percentile for the 187 'unknown' patches of each lamination

Lamination (thickness) µm	**Initial** (uncoated to coated) $\bar{x}\,\Delta E_{00}$	p = 0.9	**Heuristic** (coated to predicted) $\bar{x}\,\Delta E_{00}$	p = 0.9	**ANN** (coated to predicted) $\bar{x}\,\Delta E_{00}$	p = 0.9
42	3.4	5.3	1.3	2.2	0.7	1.2
75	3.4	5.2	1.3	2.1	0.5	0.8
125	3.6	5.3	1.7	2.6	0.7	1.3

Predictions made by the ANN are quite close to the actual measured coated patches and show colour deviations of < 1 ΔE_{00}. Averaged over all 561 predicted spectra, a mean prediction accuracy of 1.4 ΔE_{00} for the heuristic approach and 0.6 ΔE_{00} for the ANNs prediction can be attained.

Table 4 presents relevant colorimetric data including initial colour shifts and prediction results for both methods. In addition to the arithmetic mean values, the 90th percentiles p are given to allow a further evaluation of the results.

4. Discussion

Significant colour shifts can be seen, which tend to have their maximum at colours of medium brightness. Among other optical effects, the colour shifts are presumably caused by interreflections between ink or paper white surface and lamination. In darker colours, the greater initial absorption and the absence of paper white leads to a smaller light potential for multiple reflections compared to middle-toned colours. This effect slightly reverses at colours of high brightness since they have only low absorptions and therefore multiple reflections have reduced impacts. Good prediction results with mean colour deviations of < 2 ΔE_{00} are demonstrated for both approaches. Looking at the heuristic approach (Figure 7), a poor prediction accuracy for paper white reflection spectra is revealed. The reason for this lies in the calculation method of this approach as the transmission $T(\lambda)$ in Equation [8] for blank substrates is 1 due to the absence of ink. Therefore, the correcting exponent n is ineffective and a prediction is not possible.

With mean accuracies of 0.6 ΔE_{00}, the ANN shows spectral predictions with only slight deviations to the actual measured spectra, which are even hardly perceivable for human observer. Here it should be mentioned that phenomena of overfitting can be ruled out since predictions were made for test data sets which are completely unknown to the ANN until then. The prediction of a numerical series, as it was done in the present case, basically means to solve a regression problem which is a common application for this kind of ANNs. Nevertheless, the accuracy achieved seems to be impressive in their own right. In the past, many physically reasonable models and associated colorimetric calculations were developed. Using an ANN is a fundamentally different way to calculate or converte colours as it does not rely on the current technical or physical backgrounds of phenomena but on training based on known examples. One does not need to comprehend a process with all its parameters entirely and yet can achieve useful results, as is demonstrated in this paper with nearly matching spectral predictions. Based on initial lamination-induced colour shifts and obtained prediction accuracies for different approaches found in literature (cf. the introduction) and in this paper, it seems conceivable that a suitable ANN provides better results than existing physically grounded mathematical models. This hypothesis requires further investigation to prove or disprove it. It must be clear, however, that good results can only be expected for the process parameters represented by the training data set. In this investigation, only one type of lamination was examined. Other lamination materials may have different refraction indices and transmission quantities and, therefore, other influences on colour appearance. Consequently, this ANN should be retrained with suitable training data to make predictions for other lamination and print parameters.

Future work in this field could implement laminations with different parameters (e.g. refraction index, thickness) as additional input channels in a multimodal ANN to find out if a generalised network for colour shift prediction is possible. As most computing work is needed for an ANN's training, the actual utilisation of an already trained ANN has comparably low needs for computing power and provides instantaneous outcomes. The ANNs offer great potential for process improvement in a broad field of applications, including in print and media technologies – it should be easy for an expert reader to imagine other application cases. The availability and constant further development of machine learning environments and technologies also contribute to a practical implementation in e.g. colour science, colour management or quality control systems for dealing with existing and future problems.

5. Conclusions

Notable lamination-induced colour shifts of 3.46 mean ΔE_{00} were identified and spectrally predicted using two different approaches. The heuristic approach represented the lamination-induced effects on reflection spectra for colours quite well and made predictions with an accuracy of 1.43 mean ΔE_{00}, but always requires the nominal area coverages. It can be concluded, however, that this approach still has potential for improvements to enable not only prediction of colour, but also of paper white after lamination. The ANN performed equally well on average for all kind of spectra and provided an accuracy of 0.63 mean ΔE_{00} between predictions and actual measured spectra. The heuristic approach requires the fitting of only two variables whereas the ANN's training with fitting of 2 592 variables (36 × 36 × 2) requires significantly more computing effort. However, once implemented and set up, both offer immediate predictions. For a further validation of both approaches and possible scenarios for implementation, future investigations should take different lamination and print configurations into account – e.g. matte laminations, varnishes, other substrates and screenings as well. We have indications that the heuristic approach is applicable even with only a few tens of spectra for fitting, but this must be examined more closely in a future work. Another challenge is to establish and to train an ANN that is able to predict spectra for various lamination and coating scenarios with only minor adjustments. In general, ANNs offer great potential for process improvement in a broad field of applications.

References

Kleeberg, D., Süßl, F., von Oeynhausen, R., Hoffstadt, H, Seitz, J., Hansen, M., Hebes, T., Drümmer, O., Willfahrt, R., Wipperfürth, F. and Totzauer, W., 2018. *MediaStandard Print 2018: technical guidelines for data, proof and production run printing.* Berlin: Bundesverband Druck und Medien e.V. [pdf] Available at: <https://www.bvdm-online.de/fileadmin/user_upload/bvdm_MediaStandard_Print_2018.pdf> [Accessed December 2019].

Childers, A., Etheredge, A., Flannery, S. and Freeman, J., 2008. Effects of varnish on printed materials, *Flexo Global,* 1(4), pp. 20–30.

Chollet, F., 2018. *Deep Learning mit Python und Keras.* Frechen, Germany: Mitp Verlag.

Galić, E., Ljevak, I. and Zjakić, I., 2015. The influence of UV varnish on colorimetric properties of spot colors. *Procedia Engineering*, 100, pp. 1532–1538. https://doi.org/10.1016/j.proeng.2015.01.525.

Gemeinhardt, J., Saba, S. and Skoczowski, R., 2009. *Einfluss der Lackierung auf das farbliche Aussehen eines Offsetdrucks auf Papier und Karton (Fogra-Forschungsbericht Nr. 32.152),* München: Fogra Forschungsgesellschaft Druck e.V.

Hagan, M.T., Demuth, H.B., Beale, M.H. and De Jesus, O., 2014. *Neural network design.* 2nd ed. Wrocław: Amazon Fulfillment Poland Sp. z o.o.

Hébert, M., Emmel, P. and Hersch, R.D., 2002. A prediction model for reflection on varnished metallic plates. In: *Conference on Colour in Graphics, Imaging, and Vision: CGIV 2002 Proceedings*. Poitiers, France, 2–5 April 2002. Springfield, VA, USA: IS&T, pp. 453–458.

Hoffstadt, J., 2004. Simulating color changes due to coating of offset prints. In: *Conference on Colour in Graphics, Imaging, and Vision: CGIV 2004 Proceedings.* Aachen, Germany, 5–8 April 2004. Springfield, VA, USA: IS&T, pp. 489–493.

International Organization for Standardization / International Commision on Illumination, 2014. *ISO/CIE 11664-6:2014, Colorimetry – CIEDE2000 Colour-difference formula.* Geneva, Switzerland: ISO.

Selle, S., 2018. *Künstliche Neuronale Netzwerke und Deep Learning.* Saarbrücken: Hochschule für Technik und Wirtschaft des Saarlandes.